Deleterious Effects of Halides and Solvents on the Integrity of Copper Iodide Hole Extraction Layers in Hybrid Perovskite Photovoltaics

*Emily C. Smith, D. Venkataraman**

Department of Chemistry, University of Massachusetts Amherst, Amherst, Massachusetts 01003, United States

Abstract

Copper iodide (CuI) is a promising material for use as a hole transport layer in perovskite solar cells due to its optical transparency, low-cost fabrication, and efficient electronic (hole) conductivity. Various reports of perovskite solar cells that utilize CuI have shown impressive solar cell performance and improved device stability. Despite these observations, we found no clear experimental evidence that the CuI hole transport layer is retained in perovskite p-i-n solar cells after device fabrication. Using powder X-ray diffraction (PXRD), UV-vis spectroscopy, and impedance spectroscopy, we studied how each of the components present in the precursor solution for fabricating the perovskite active layer impacts the integrity of CuI films. Based on these data, we establish the deleterious effects of halide ions and solvents such as dimethyl sulfoxide (DMSO). We also show that we can fabricate stable CuI material *in situ* during perovskite deposition by taking advantage of a known redox chemistry of Cu(II)/Cu(I) and halides.

Introduction

Copper(I) iodide (CuI) is an intrinsic p-type semiconductor[1, 2] with high hole mobility.[1, 3-5] It is optically transparent and can be fabricated as thin films using solution-based techniques.[5, 6] As such, CuI has been successfully employed in various electronic devices including organic photovoltaics,[7, 8] light emitting diodes,[9, 10] and thin film transistors.[6, 11] Several reports have shown that CuI as hole transport layer (HTL) in perovskite-based photovoltaic devices, particularly in an inverted planar p-i-n device architecture, enhances power conversion efficiency.[12-19] CuI HTLs have also been shown to improve charge extraction, thus, enhancing light stability of perovskite solar cells.[12, 13, 15, 17-20] For these reasons, CuI is a widely studied as a HTL to achieve highly efficient and stable perovskite-based electronic devices.

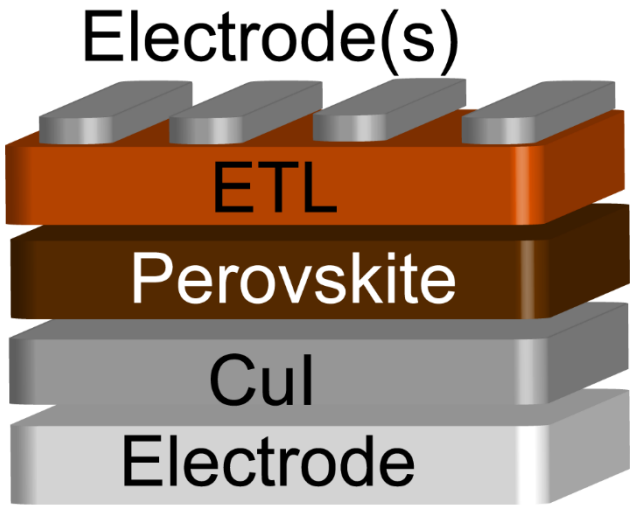

Figure 1. Schematic of a perovskite solar cell in the p-i-n configuration. CuI is shown as the hole transport layer (bottom layer). The electron transport layer is above the perovskite and is typically a functionalized C_{60}.

In the p-i-n architecture (Figure 1), CuI constitutes the bottom layer in the device, thus, is exposed to the deposition conditions of the layers above it during film fabrication, including the perovskite active layer. In many reports, the presence of the CuI layer is not unequivocally established.[12-19] Thus, some reports have questioned the presence of a CuI layer, particularly in p-i-n devices fabricated via solution.[21] Using powder X-ray diffraction, UV-vis spectroscopy, and impedance spectroscopy, we studied how each of the components present in the precursor solution for fabricating the perovskite active layer impacts the integrity of CuI films. Using these data, we establish the deleterious effects of halide ions and solvents such as DMSO. We also show that we can fabricate stable CuI material *in situ* during perovskite deposition by taking advantage of a known redox chemistry of Cu(II)/Cu(I) and halides.

Experimental Section

Sample fabrication. Thin films were deposited through spin coating onto either glass or indium doped tin oxide (ITO) coated glass substrates. All precursor solutions and sample films were fabricated inside a nitrogen-filled glovebox (<0.1 ppm O_2, <0.1 ppm H_2O) with exception of the copper(II) acetate (CuOAc) layer, which was prepared under ambient conditions. Substrates were cleaned via sequential sonication in soap solution, water, acetone, and isopropanol for 20 min each then dried in an oven at 140 ºC for at least 2 h. The cleaned substrates were then treated with UV-ozone for 20 min before spin coating.

The CuI layer was fabricated as follows: A solution of CuI was prepared in acetonitrile (15 mg mL^{-1}) by stirring CuI in acetonitrile at room temperature until CuI was fully dissolved (~12 h). This CuI solution was then deposited onto the substrate (50 μL) via spin coating at 3000 rpm for 30 s. The thin films were annealed on a hot plate at 100 ºC for 10 min before the deposition of the next layer. The resulting thickness of the films were ~40 – 50 nm measured by profilometry.

For samples treated with CuOAc, the procedure is as follows: A 5 mg mL^{-1} solution of CuOAc in isopropanol was prepared by stirring CuOAc in isopropanol at room temperature overnight. The undissolved solid was filtered using a 0.45 μM PTFE syringe filter. The solution was then deposited on top of the CuI films (50 μL) via spin coating at 1000 rpm for 60 s. The films were annealed in an oven at 110 ºC for 30 min.

The perovskite layer was fabricated as follows: A 1.4 M precursor solution was prepared by adding methylammonium iodide (0.7 M) and PbI_2 (0.7 M) to a cosolvent mixture of γ-butyrolactone (GBL) in dimethyl sulfoxide (DMSO) (*v/v* 7:3). Some experiments required a cosolvent mixture containing *N*,*N*-dimethylformamide (DMF). In this case, methylammonium and lead iodide salts were dissolved in a cosolvent mixture of DMF in DMSO (*v/v* 8:2). The solutions were allowed to stir overnight at 50 ºC. The solution was deposited onto the substrates (50 μL). In the case of the GBL cosolvent system, the substrate was spun at 1500 rpm for 10 s, then 2000 rpm for 60 s. When 40 s remained in the total spinning cycle a chlorobenzene antisolvent (100 μL) was dripped onto the substrate. In the case of the DMF cosolvent system, the substrate was spun at 2000 rpm for 10 s, then 6000 rpm for 30 s. When there was 20 s left in the spinning procedure a chlorobenzene antisolvent (100 μL) was dropped onto the substrates. The films were annealed on a hotplate at 100 ºC for 5 min.

Characterization. Powder X-ray diffraction experiments were run using a Rigaku SmartLab SE X-ray diffractometer. Scans were collected from 10º – 55º 2θ at a step size of 0.010º and at a rate of 20º/step using X-ray fluorescence reduction. Conductivity measurements were conducted using a Solartron Analytical Electrochemical Impedance Analyzer setup with an SI 1287 electrochemical interface and a 1252A frequency response analyzer. Samples were scanned from 100,000 – 10 Hz at an oscillation amplitude ranging from 50 – 100 mV. To determine resistance

from impedance results, the data were fitted to an equivalent circuit model consisting of two R-C circuits in series (Figure S1), and the sum of the resistance was taken as an estimate for composite resistance of the sample. ZView (Scribner Associates) was used as a fitting software. UV-vis absorption measurements were run on solid films using a Shimadzu UV-2401PC spectrophotometer. Data was collected between 325 – 600 nm.

Results & Discussion

A typical precursor solution for perovskites is composed of lead halides, and alkylammonium halides such as methylammonium iodide (MAI) dissolved in solvents such as γ-butyrolactone (GBL), *N*,*N*-dimethylformamide (DMF), and dimethyl sulfoxide (DMSO). When we fabricated a prototypical hybrid perovskite, methylammonium lead triiodide ($MAPbI_3$), using MAI/PbI_2 over a thin film of CuI, the powder X-diffraction (PXRD) pattern did not show peaks attributable to CuI (Figure 2). This observation is consistent with many reports that contain the absence of peaks related to CuI in the PXRD.[13-15, 18, 19] Often the lack of peaks from CuI is attributed to the dominance of the peaks from the perovskite.[13]

To understand the lack of peaks related to CuI, we first assessed the influence of perovskite precursor solvents on the optical, electrical, and structural properties of the CuI films. In these studies, we used common perovskite precursor solvents: GBL, DMF, and DMSO, and two cosolvent mixtures of GBL:DMSO (*v/v* 7:3) and DMF:DMSO (*v/v* 8:2). We then exposed the CuI films to these solvents by spin coating them onto a film of CuI using the same conditions for perovskite fabrication. The CuI films were then annealed at 100 ºC for 5 min before further characterization.

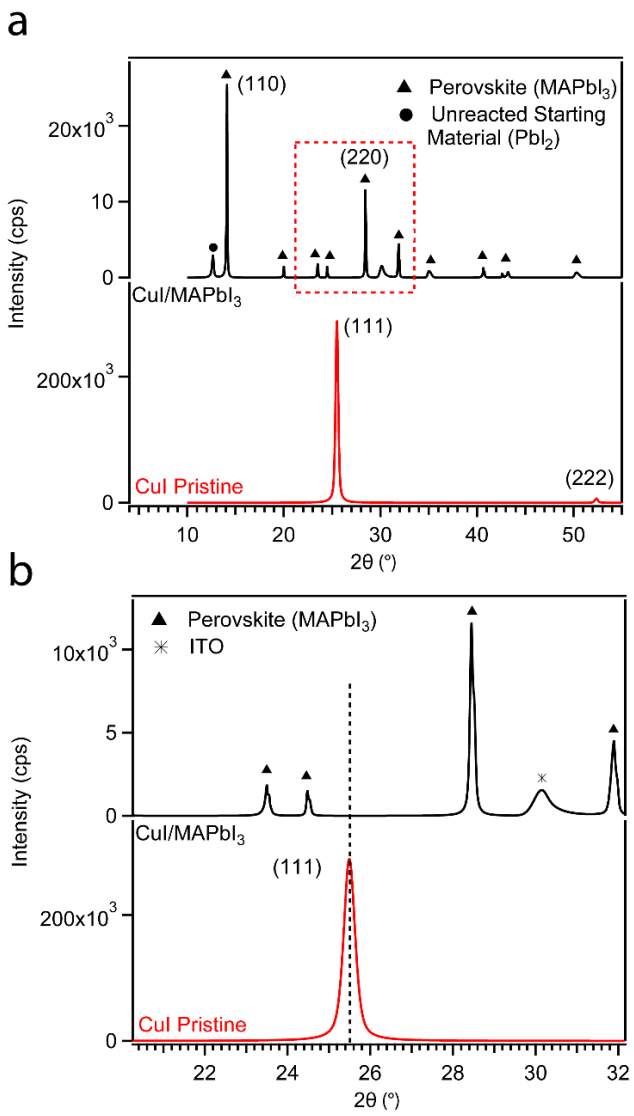

Figure 2. (A) Powder X-ray patterns for CuI films before (red) and after (black) deposition of perovskite on top. Red dashed box shows region of interest where CuI and ITO peaks appear; (B) the powder X-ray pattern from (A) has been zoomed into on the region between 20.2 – 32.1° 2θ to show the lack of CuI diffraction and the appearance of the ITO peak.

We characterized the optical properties of films before and after solvent treatment with UV-vis spectroscopy. A representative UV-vis spectra of a pristine film of CuI is shown in Figure S2. The films have a sharp absorption edge occurring at 420 nm. Tauc analysis indicates a band gap of 2.98

eV (Figure S2). This is consistent with reported band gaps of CuI thin films processed in acetonitrile.[6, 11] We then characterized the films after treating them with common perovskite precursor solvents. Films treated with DMF or GBL both showed little to no change in the absorbance, indicating minimal effect of these solvents on the optical properties of these films (Figure 3). The lack of change in the absorbance also indicates that the thickness of the CuI films remains unaltered as well. Films treated with DMSO, however, showed no peak around 420 nm. We found that CuI was soluble in DMSO (Figure S3), thus, we hypothesized this result may be due to the CuI films dissolving and being washed away during the spin coating step. Films that were treated with the cosolvent mixtures of GBL:DMSO and DMF:DMSO showed a decrease in absorbance relative to the untreated films (Figure S3). These observations are consistent with the hypothesis that DMSO may be dissolving the CuI films under the film fabrication conditions.

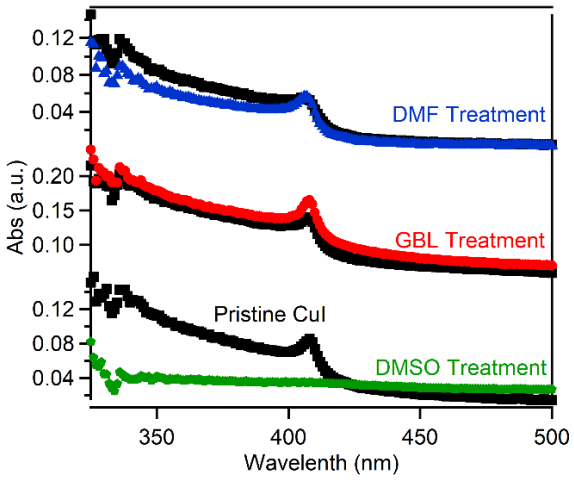

Figure 3. UV-vis spectra of a pristine CuI film before (black) and after (colored) treatment with DMF (blue), GBL (red), and DMSO (green)

Next, we measured the electrical conductivity of the CuI films before and after solvent treatment using impedance spectroscopy. We measured films in a lateral configuration by depositing them on top of prepatterned ITO coated substrates. In this measurement, an AC voltage is applied to the

sample and the resulting AC current is measured. By convention, the data is plotted in a complex plane called a Nyquist plot. The data can then be fitted to established equivalent circuit models to extract parameters such as resistance and capacitance. In our samples, we observed a common impedance response consisting of two semicircles, observed in various semiconductor and ionically conducting materials and devices. To analyze the impedance data, we used a standard equivalent circuit model.[22-28] We took the sum of all resistive elements to represent an estimate for the composite resistance of the CuI films. The Nyquist plots of CuI films before and after solvent treatment can be found in Figure S4. The relevant equivalent circuit model used in this work can be found in Figure S1. Pristine CuI films showed electrical resistance of 513 ± 42 Ω. We found the resistance of the films increased after the annealing step. After treatment with GBL, we did not observe any experimentally significant change in the resistance of the films. When the films were treated with DMF, there was a marked increase in the resistance of the films ($\Delta R = 2848 \pm 35\ \Omega$). One possibility for this observation is the coordination of DMF with copper in the CuI films. It has been reported that DMF can coordinate to the surface of CuI nanoparticles.[29] We hypothesize these same interactions could result in accumulation of DMF at the surface and grain boundaries of the films which could cause in an increase in the overall film resistance. Regardless, the retention of an impedance signal in these samples indicated the CuI films remained intact during DMF treatment and that the interaction between DMF and CuI was likely minimal in these conditions. In films exposed to DMSO, however, there was no measurable impedance response. This is consistent with the loss of absorbance in UV-vis spectra in films treated with DMSO.

We characterized the CuI films before and after solvent treatment using powder X-ray diffraction (PXRD). An example of the PXRD pattern for a pristine film of CuI can be found in Figure 4. We observed films that were highly oriented along (111), consistent with reports for CuI thin films.[6,

[11, 19] After treatment with DMF and GBL, we observed that the PXRD pattern of the CuI films remained mostly unchanged (Figure 4a). For these films, we observed a slight increase in the intensity of the (111) peak, which was consistent with untreated control films taken before and after the temperature annealing step. Scherrer analysis demonstrated that the increasing diffraction intensity after the annealing step corresponded to a ~56% increase in the crystalline grain size of the film (from ~17 nm to ~26 nm, when the shape factor k = 0.94). For films treated with pure DMSO, we observed a total loss of diffraction peaks, consistent with the removal of crystalline CuI material from the substrate (Figure 4a). For CuI films treated with the cosolvent mixtures, we observed a reduction in the intensity of the diffraction peaks but did not observe a complete removal of the signal (Figure 4a). The PXRD results were consistent with the absorption and conductivity results.

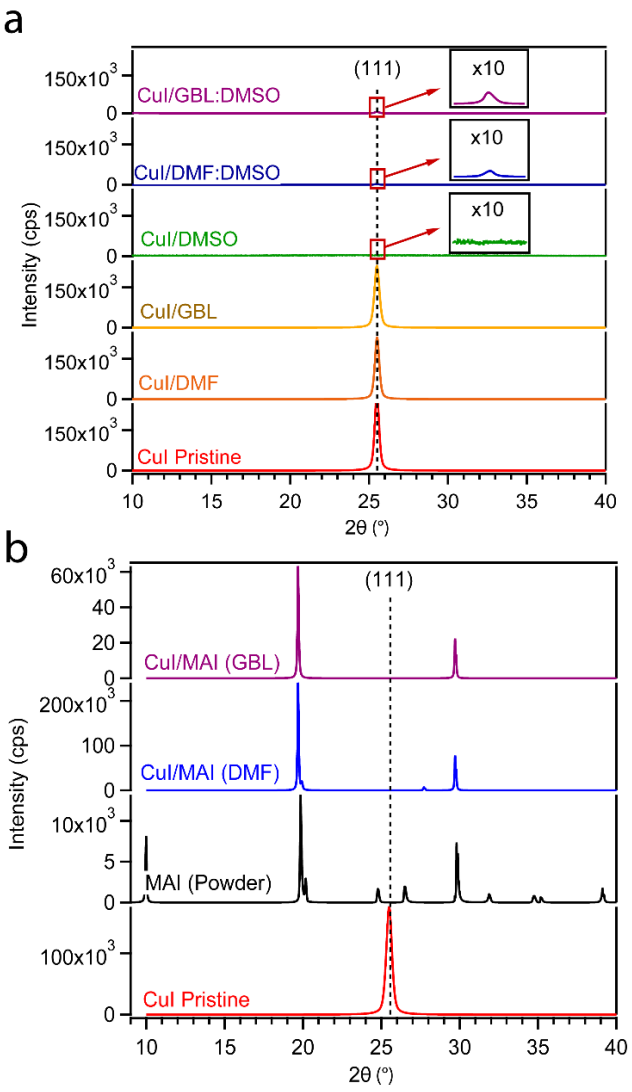

Figure 4. (A) Powder X-ray patterns for CuI films before (red) and after solvent treatment with DMF (orange), GBL (yellow), DMSO (green), and cosolvent mixtures of DMF:DMSO (blue), and GBL:DMSO (purple); (B) Powder X-ray patterns for CuI after treatment with a salt solution of MAI in DMF (blue) and GBL (purple). For reference, pristine CuI (red) and experimental MAI powder (black) are shown.

Taken together, the data suggest that DMSO may be dissolving CuI films. Our data also suggests that solvents such as DMF can alter the conductivity of hole transport materials, altering the efficiency of charge extraction and thus the efficiency and stability of photovoltaic devices.

To elucidate the effects of the salts on CuI film characteristics, we treated the CuI films with salt solution via spin coating. We focused on methylammonium iodide (MAI) and PbI_2, which are commonly used to fabricate $MAPbI_3$, the archetypical perovskite active layer. We found that PbI_2 was insoluble in GBL, and therefore we cannot determine the impact of PbI_2 alone in that solvent. In DMF, we observed the results of PbI_2 solutions were consistent with those of MAI solutions, thus, we chose to focus our discussion on just the MAI solutions. We prepared 0.7 M solutions of MAI in either pure GBL or DMF. We chose to omit the addition of DMSO in these studies since this solvent interfered with the CuI film characteristics in our previous study. By using only GBL and DMF, we can better asses the influence of only the iodide salt on the CuI film characteristics.

In UV-vis studies we observed that when we treated CuI films with solutions of MAI in either GBL or DMF, there was a total loss of absorbance associated with the CuI films (Figure S5). Conductivity studies also corroborated the findings of the UV-vis results; films treated with MAI in GBL or DMF (Figure S6) did not show any impedance response. This contrasts with our earlier observation that CuI films treated with pure GBL or DMF retained absorbance and impedance response.

PXRD of CuI films treated with MAI in either GBL or DMF (Figure 4b) did not show peaks associated with CuI. To check if the diffraction from the MAI film attenuates the diffraction from the CuI film, we prepared samples on a conducting substrate coated with indium doped tin oxide (ITO). The ITO substrate has a weak diffraction peak at 30.2º 2θ which corresponds to diffraction of the (222) plane.[30] For reference, the experimentally matched PXRD profile for a control film of

ITO coated on a glass substrate is shown in Figure S7.[30] First, we deposited a film of CuI onto an ITO coated substrate. On top of the CuI film, we fabricated a film of hybrid perovskite ($MAPbI_3$) from a precursor solution containing MAI, PbI_2, and a cosolvent mixture of GBL:DMSO (*v/v* 7:3). The PXRD of these samples shows a peak attributable to ITO but not CuI (Figure 2a,b). Thus, we conclude that dissolution and not signal attenuation is the cause for the lack of CuI peaks in the PXRD.

It is well-known that CuI can react with I^- to form a soluble anion, $[CuI_2]^-$ (Scheme 1).[31] It is a similar reaction that allows the dissolution of PbI_2 in the presence of iodide salts. Our studies establish that the implicit assumption that I^- and DMSO cannot dissolve CuI films on time scales of perovskite fabrication is incorrect.

Scheme 1. Addition-Elimination reaction of CuI and aqueous I^- in excess

$$CuI_{(s)} + I^- \longrightarrow [CuI_2]^-$$

As our work was in progress, a report by Grishko *et al.* was published that also concluded that CuI 'gets dissolved if halide perovskites are deposited atop from solutions…'.[21] While their conclusion is like ours, they noted that CuI was not soluble in DMSO and attributed the dissolution to the presence of I^- and methylammonium ions. Our data shows that DMSO can indeed dissolve CuI films, and the dissolution of films in iodide-rich solutions is exclusively from the reaction of the I^- ions with CuI to form $[CuI_2]^-$, which is soluble in many organic solvents. Grishko *et al.* concluded that a 'CuI/[$MAPbI_3$] heterojunction cannot be obtained using the solution-deposition of [$MAPbI_3$]' and showed that vapor deposition of metallic lead followed by its conversion to $MAPbI_3$ by reacting with polyiodide melts prevents the dissolution CuI films. Solution processing of hybrid perovskite is a principal feature that makes attractive for fabricating thin film solar cells

at low-cost. Therefore, we reasoned that we need a method that conserves the capability to use solution-processing and protects the CuI films from being etched by the I^- rich perovskite solution.

It is well-established that Cu(II) salts can be reduced to Cu(I) by I^-.[31] This redox reaction is used in the synthesis of CuI and is the basis for estimating Cu(II) via iodometric titrations.[32] Thus, this reaction provides a potential route for *in situ* fabrication of CuI using the I^- present in the perovskite precursor solution. To test this possibility, we prepared layered samples starting with a film of CuI, followed by a layer of copper(II) acetate (CuOAc). Then we exposed these films to solutions of MAI dissolved in GBL, or MAI and PbI_2 dissolved in the cosolvent system GBL:DMSO to form the full perovskite layer. We expected that the CuOAc will react with MAI salt to form CuI. Thus, I^- in the precursor solution will be used to form CuI instead of etching it.

Scheme 2. Reaction of copper(II) acetate with methylammonium iodide

$$2\ Cu(CH_3COO)_2 + 4\ I^- \longrightarrow 2\ CuI + I_2 + 4\ CH_3COO^-$$

A schematic of the fabricated device is shown in Figure 5a. Like prior experiments, we treated the CuI/CuOAc layered samples by spin coating the salt solutions on top using the same conditions which we use during perovskite fabrication. We observed that films with a layer of CuOAc turned reddish-brown on exposure to the salt solution of MAI (Figure S8) indicating the formation of iodine. Control films with no CuOAc did not show this color change. The brown color was transient and sublimed on heating, consistent with the formation of iodine.

We then characterized these films using UV-vis spectroscopy. First, we measured the absorption of a CuI film before and after layering the CuOAc layer on top. We observed that the addition of the CuOAc layer on top of CuI had minimal effect on the optical properties of the film, most likely because CuOAc absorption is most intense between 550 – 800 nm and there is minimal absorption

at 420 nm where we observe the CuI absorption edge (Figure S9). Next, we treated the CuI/CuOAc layered samples with a solution of MAI in GBL. We found that there was a weak absorption at 420 nm in these samples, which is consistent with the expected formation of CuI (Figure S10).

Next, we measured the electrical properties of the samples. We observed films increased in resistance after the temperature annealing step at 100 ºC for 30 min, otherwise, there was no significant change in the resistance of the CuI films after the CuOAc deposition (Figure S11). The CuOAc layered films were then treated with a solution of MAI in GBL. We observed a loss of signal for these samples, similar to control samples which had not been treated with CuOAc (Figure S11). From this result, we surmise that the film of CuI may be patchy and not electrically continuous.

We then measured the PXRD of CuI films before and after the coating of the CuOAc layer. We did not observe any significant changes in the CuI film diffraction, indicating that the that the CuOAc layer does not disrupt the crystalline packing of the CuI film. We also did not observe any diffraction peaks corresponding to CuOAc (Figure S12). This indicates that the CuOAc layer is either amorphous or too thin to have enough signal or both. Next, we treated the layered CuOAc samples with solutions of MAI in GBL. We observed that the diffraction peak corresponding to the CuI layer at 25.5º 2θ was retained in samples that contained CuOAc (Figure 5b). In control samples which only contained CuI, the diffraction peak corresponding to this material disappeared after treatment with the MAI solution. Additionally, we observed that there was a retention of the CuI diffraction even after exposure to the full perovskite precursor solution including both MAI and PbI_2 as well as the GBL:DMSO cosolvent (Figure 5b).

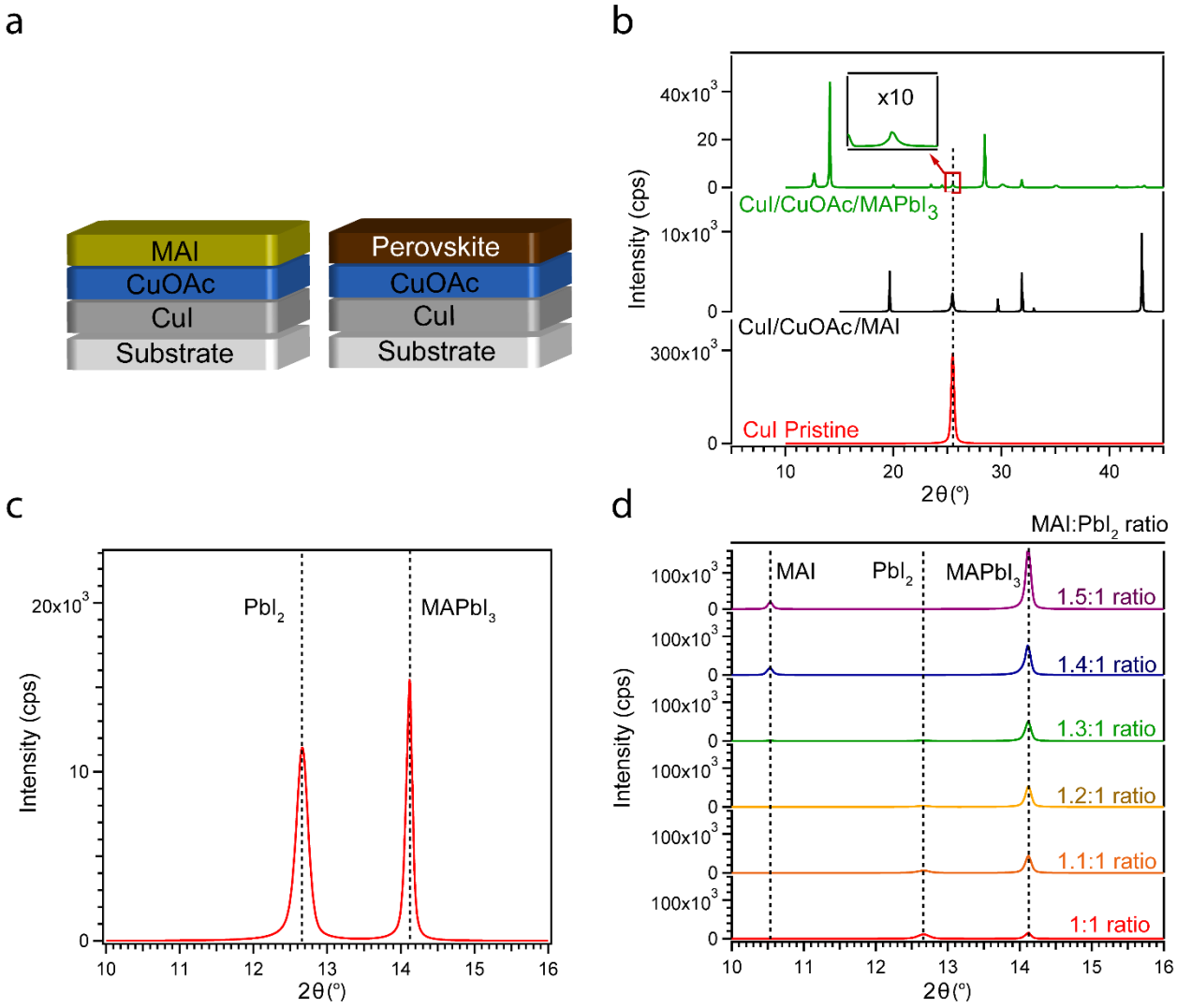

Figure 5. (A) Schematic of layered devices tested in these studies showing a CuOAc layer placed between the CuI layer and the perovskite or MAI; (B) PXRD patterns of layered device containing CuOAc after treatment with MAI (black) and $MAPbI_3$ perovskite (green) showing the retention of the crystalline CuI peak after treatment; (C) PXRD pattern of $MAPbI_3$ film deposited onto a CuOAc layer showing a high quantity of unreacted PbI_2 in the films; (D) PXRD pattern of $MAPbI_3$ films with varying ratios of MAI:PbI_2 deposited on top of a CuOAc layer.

We observed that the perovskite films that were deposited on top of the CuOAc layer contained a large quantity of unreacted PbI_2 (Figure 5c). In these precursor solutions, MAI and PbI_2 were added in a stoichiometric ratio. This observation is consistent with our expectation that I^- are also used to convert CuOAc to CuI. We then varied the ratio of MAI to PbI_2 in the precursor solution to minimize the amount of unreacted PbI_2 in the resulting films (Figure 5d). We found the optimal ratio of MAI:PbI_2 to be 1.2:1 for films deposited on top of CuOAc under our fabrication conditions. Overall, this result confirms that a layer of CuOAc in between the CuI and the perovskite can be used to preserve crystalline CuI material in the presence of the I^- rich solution and DMSO.

Conclusions

Taken together, our studies show if CuI is used as a hole transport material in p-i-n perovskite solar cells, then the fabrication of the active layer can impact the integrity of the HTL. We show that the CuI films dissolve in DMSO, a component of the active layer precursor solution, during active layer fabrication. Additionally, the electrical conductivity of CuI is altered by the use of DMF as a solvent, which may impact the charge extraction in full photovoltaic devices. Furthermore, CuI thin films undergo an addition-elimination reaction with I^- in the perovskite precursor solutions, which results in dissolution and removal of that layer during perovskite fabrication. We showed that we can preserve crystalline CuI material in devices under these conditions by applying fundamental copper chemistry. Herein, we showed the efficacy of the use of copper(II) acetate as an interlayer that can work to preserve crystalline CuI during perovskite solar cell fabrication. Full characterization and optimization of this system, especially in the context of solar cell devices, is the subject of ongoing research and our results will be reported in due time.

ACKNOWLEDGMENT

The acquisition of the powder X-ray diffractometer was made possible through the National Science Foundation Major Research Instrumentation Program (CHE-1726578). This work was supported in part by a Graduate School Research Grant from the University of Massachusetts Amherst. We gratefully acknowledge the financial support of the US Army CCDC Solider Center through contract no. W911QY1820002 for this work. We gratefully acknowledge Hamza Javaid for his help in the acquisition of the CuI film thickness.

ASSOCIATED CONTENT

Supporting Information.

Supplementary UV-vis, powder X-ray diffraction, and conductivity measurements. Equivalent circuit model used for resistance calculations. (PDF)

The following files are available free of charge via the Internet at http://pubs.acs.org.

AUTHOR INFORMATION

Corresponding Author

D. Venkataraman – Department of Chemistry, University of Massachusetts Amherst, Amherst, MA 01003; http://orcid.org/0000-0003-2906-0579; Email: dv@umass.edu

Authors

Emily C. Smith – Department of Chemistry, University of Massachusetts Amherst, Amherst, MA 01003; https://orcid.org/0000-0002-0849-897X

Notes

The authors declare no competing financial interest.

REFERENCES

1. Wang, J.; Li, J. B.; Li, S. S. Native p-type transparent conductive CuI via intrinsic defects. *J. Appl. Phys.* **2011,** 110, 5.

2. Coroa, J.; Faustino, B. M. M.; Marques, A.; Bianchi, C.; Koskinen, T.; Juntunen, T.; Tittonen, I.; Ferreira, I. Highly transparent copper iodide thin film thermoelectric generator on a flexible substrate. *Rsc Advances* **2019,** 9, 35384-35391.

3. Chen, D. G.; Wang, Y. J.; Lin, Z.; Huang, J. K.; Chen, X. Z.; Pan, D. M.; Huang, F. Growth Strategy and Physical Properties of the High Mobility P-Type CuI Crystal. *Cryst. Growth Des.* **2010,** 10, 2057-2060.

4. Yamada, N.; Ino, R.; Ninomiya, Y. Truly Transparent p-Type gamma-CuI Thin Films with High Hole Mobility. *Chem. Mat.* **2016,** 28, 4971-4981.

5. Inudo, S.; Miyake, M.; Hirato, T. Electrical properties of CuI films prepared by spin coating. *Phys. Status Solidi A-Appl. Mat.* **2013,** 210, 2395-2398.

6. Liu, A.; Zhu, H. H.; Park, W. T.; Kang, S. J.; Xu, Y.; Kim, M. G.; Noh, Y. Y. Room-Temperature Solution-Synthesized p-Type Copper(I) Iodide Semiconductors for Transparent Thin-Film Transistors and Complementary Electronics. *Adv. Mater.* **2018,** 30, 7.

7. Das, S.; Choi, J. Y.; Alford, T. L. P3HT:PC61BM based solar cells employing solution processed copper iodide as the hole transport layer. *Sol. Energy Mater. Sol. Cells* **2015,** 133, 255-259.

8. Peng, Y.; Yaacobi-Gross, N.; Perumal, A. K.; Faber, H. A.; Vourlias, G.; Patsalas, P. A.; Bradley, D. D. C.; He, Z. Q.; Anthopoulos, T. D. Efficient organic solar cells using copper(I) iodide (CuI) hole transport layers. *Appl. Phys. Lett.* **2015,** 106, 4.

9. Ahn, D.; Song, J. D.; Kang, S. S.; Lim, J. Y.; Yang, S. H.; Ko, S.; Park, S. H.; Park, S. J.; Kim, D. S.; Chang, H. J., *et al.* Intrinsically p-type cuprous iodide semiconductor for hybrid light-emitting diodes. *Sci Rep* **2020,** 10, 8.

10. Stakhira, P.; Cherpak, V.; Volynyuk, D.; Ivastchyshyn, F.; Hotra, Z.; Tataryn, V.; Luka, G. Characteristics of organic light emitting diodes with copper iodide as injection layer. *Thin Solid Films* **2010,** 518, 7016-7018.

11. Liu, A.; Zhu, H. H.; Park, W. T.; Kim, S. J.; Kim, H.; Kim, M. G.; Noh, Y. Y. High-performance p-channel transistors with transparent Zn doped-CuI. *Nat. Commun.* **2020,** 11, 8.

12. Saranin, D.; Gostischev, P.; Tatarinov, D.; Ermanova, I.; Mazov, V.; Muratov, D.; Tameev, A.; Kuznetsov, D.; Didenko, S.; Di Carlo, A. Copper Iodide Interlayer for Improved Charge Extraction and Stability of Inverted Perovskite Solar Cells. *Materials* **2019,** 12, 14.

13. Hu, W. D.; Dall'Agnese, C.; Wang, X. F.; Chen, G.; Li, M. Z.; Song, J. X.; Wei, Y. J.; Miyasaka, T. Copper iodide-PEDOT:PSS double hole transport layers for improved efficiency and stability in perovskite solar cells. *J. Photochem. Photobiol. A-Chem.* **2018,** 357, 36-40.

14. Javaid, H.; Duzhko, V. V.; Venkataraman, D. Hole Transport Bilayer for Highly Efficient and Stable Inverted Perovskite Solar Cells. *ACS Appl. Energ. Mater.* **2021,** 4, 72-80.

15. Chen, W. Y.; Deng, L. L.; Dai, S. M.; Wang, X.; Tian, C. B.; Zhan, X. X.; Xie, S. Y.; Huang, R. B.; Zheng, L. S. Low-cost solution-processed copper iodide as an alternative to PEDOT:PSS hole transport layer for efficient and stable inverted planar heterojunction perovskite solar cells. *J. Mater. Chem. A* **2015,** 3, 19353-19359.

16. Sun, W. H.; Ye, S. Y.; Rao, H. X.; Li, Y. L.; Liu, Z. W.; Xiao, L. X.; Chen, Z. J.; Bian, Z. Q.; Huang, C. H. Room-temperature and solution-processed copper iodide as the hole transport layer for inverted planar perovskite solar cells. *Nanoscale* **2016,** 8, 15954-15960.

17. Wang, H. X.; Yu, Z.; Lai, J. B.; Song, X. K.; Yang, X. C.; Hagfeldt, A.; Sun, L. C. One plus one greater than two: high-performance inverted planar perovskite solar cells based on a composite CuI/CuSCN hole-transporting layer. *J. Mater. Chem. A* **2018,** 6, 21435-21444.

18. Khadka, D. B.; Shirai, Y.; Yanagida, M.; Miyano, K. Ammoniated aqueous precursor ink processed copper iodide as hole transport layer for inverted planar perovskite solar cells. *Sol. Energy Mater. Sol. Cells* **2020,** 210, 7.

19. Wang, H. X.; Yu, Z.; Jiang, X.; Li, J. J.; Cai, B.; Yang, X. C.; Sun, L. C. Efficient and Stable Inverted Planar Perovskite Solar Cells Employing CuI as Hole-Transporting Layer Prepared by Solid-Gas Transformation. *Energy Technol.* **2017,** 5, 1836-1843.

20. Lin, Y. Z.; Chen, B.; Fang, Y. J.; Zhao, J. J.; Bao, C. X.; Yu, Z. H.; Deng, Y. H.; Rudd, P. N.; Yan, Y. F.; Yuan, Y. B., *et al.* Excess charge-carrier induced instability of hybrid perovskites. *Nat. Commun.* **2018,** 9, 9.

21. Grishko, A. Y.; Zharenova, E. A.; Goodilina, E. A.; Tarasov, A. B. Solvent-free deposition of hybrid halide perovskites onto thin films of copper iodide p-type conductor. *Mendeleev Commun.* **2021,** 31, 163-165.

22. Nobre, M. A. L.; Lanfredi, S. Grain boundary electric characterization of Zn7Sb2O12 semiconducting ceramic: A negative temperature coefficient thermistor. *J. Appl. Phys.* **2003,** 93, 5576-5582.

23. Lim, E. L.; Yap, C. C.; Jumali, M. H. H.; Khairulaman, F. L. Solution-dispersed copper iodide anode buffer layer gives P3HT:PCBM-based organic solar cells an efficiency boost. *J. Mater. Sci.-Mater. Electron.* **2019,** 30, 2726-2731.

24. Ginting, R. T.; Yap, C. C.; Yahaya, M.; Salleh, M. M. In *Impedance Spectroscopy Characterization of Inverted Type Organic Solar Cells Based on Poly(3-hexylthiophene-2,5-diyl)*, Universiti-Kebangsaan-Malaysia, Faculty-of-Science-and-Technology Postgraduate Colloquium, Univ Kebangsaan Malaysia, Fac Sci & Technol, Bangi, MALAYSIA, Jul 03-04; Amer Inst Physics: Univ Kebangsaan Malaysia, Fac Sci & Technol, Bangi, MALAYSIA, 2013; pp 29-34.

25. Mandal, S.; Menon, R. Impedance measurements in undoped and doped regioregular poly(3-hexylthiophene). *J. Phys. D-Appl. Phys.* **2020,** 53, 8.

26. Jin, M. J.; Jo, J.; Yoo, J. W. Impedance spectroscopy analysis on the effects of TiO2 interfacial atomic layers in ZnO nanorod polymer solar cells: Effects of interfacial charge extraction on diffusion and recombination. *Org. Electron.* **2015,** 19, 83-91.

27. Chen, H. W.; Huang, T. Y.; Chang, T. H.; Sanehira, Y.; Kung, C. W.; Chu, C. W.; Ikegami, M.; Miyasaka, T.; Ho, K. C. Efficiency Enhancement of Hybrid Perovskite Solar Cells with MEH-PPV Hole-Transporting Layers. *Sci Rep* **2016,** 6, 9.

28. Tian, C. B.; Castro, E.; Betancourt-Solis, G.; Nan, Z.; Fernandez-Delgado, O.; Jankuru, S.; Echegoyen, L. Fullerene derivative with a branched alkyl chain exhibits enhanced charge extraction and stability in inverted planar perovskite solar cells. *New J. Chem.* **2018,** 42, 2896-2902.

29. Zhong, Y. C.; Li, Y.; Lan, X. Y.; Wang, J.; Wang, J. N.; Zhang, Y. Enhancing Efficiency and Stability of Polymer Solar Cells Based on CuI Nanoparticles as the Hole Transport Layer. *IEEE J. Photovolt.* **2021,** 11, 668-673.

30. Nadaud, N.; Lequeux, N.; Nanot, M.; Jove, J.; Roisnel, T. Structural studies of tin-doped indium oxide (ITO) and In4Sn3O12. *J. Solid State Chem.* **1998,** 135, 140-148.

31. Cotton, F. A.; Wilkinson, G. Advanced Inorganic Chemistry a Comprehensive Text; Interscience Publishers: 1962.

32. Shaffer, P. A.; Hartmann, A. F. The iodometric determination of copper and its use in sugar analysis. I. Equilibria in the reaction between copper sulfate and potassium iodide. *J. Biol. Chem.* **1921,** 45, 0349-0364.

Table of Contents graphic